

Dissolution characteristics of sericite in chalcopyrite bioleaching and its effect on copper extraction

Ying-bo Dong, Hao Li, Hai Lin, and Yuan Zhang

School of Energy and Environmental Engineering, University of Science and Technology Beijing, Beijing 100083, China
(Received: 29 June 2016; revised: 25 July 2016; accepted: 29 August 2016)

Abstract: The effects of sericite particle size, rotation speed, and leaching temperature on sericite dissolution and copper extraction in a chalcopyrite bioleaching system were examined. Finer particles, appropriate temperature and rotation speed for *Acidithiobacillus ferrooxidans* resulted in a higher Al^{3+} dissolution concentration. The Al^{3+} dissolution concentration reached its highest concentration of 38.66 mg/L after 48-d leaching when the sericite particle size, temperature, and rotation speed were 43 μm , 30°C, and 160 r/min, respectively. Meanwhile, the sericite particle size, rotation speed, and temperature can affect copper extraction. The copper extraction rate is higher when the sericite particle size is finer. An appropriately high temperature is favorable for copper leaching. The dissolution of sericite fitted the shrinking core model, $1 - (2/3)\alpha - (1 - \alpha)^{2/3} = k_1t$, which indicates that internal diffusion is the decision step controlling the overall reaction rate in the leaching process. Scanning electron microscopy analysis showed small precipitates covered on the surface of sericite after leaching, which increased the diffusion resistance of the leaching solution and dissolved ions.

Keywords: sericite; bioleaching; copper extraction; dissolution kinetic; shrinking core model

1. Introduction

Traditional processing methods cannot effectively extract low grade mineral resources, because of high energy consumption and environmental pollution. To solve this problem, bioleaching has gradually been used on a large scale for processing minerals, particularly copper. At present, the copper extracted by the bioleaching method accounts for about 25% of the world's total copper production. Bioleaching of copper has achieved industrialization in the United States, Canada, Australia, and other more than 20 countries [1].

Gangue minerals are abundant and commonly found in copper mines and occur as two main types: oxides and silicates. Sericite exists as a gangue mineral in metallic ores and tailings. For example, copper tailings of Jiangxi Dexing contain nearly 34wt% sericite (including some illite) [2]. However, the influence of gangue minerals on copper bioleaching has not been extensively and systematically investigated either locally or internationally. Mo *et al.* [3] used mixed cultures to investigate the effect of sericite addition

and discovered that it can increase chalcopyrite bioleaching by approximately 12%. However, the main influence on chalcopyrite bioleaching is metallic ion dissolution, which not only significantly affects microorganisms but also the leaching efficiency of copper [4–5]. Fischer *et al.* [6] examined the influence of aluminum on a number of acidophilic bacteria, including *Thiobacillus ferrooxidans*. Their findings revealed that the lag phase of a batch culture cycle did not increase with the increase in aluminum concentration, unlike the cell number doubling period. Blight and Ralph [7] determined that aluminum ions do not exert any direct metabolic effect on iron oxidizing cells; however, high concentrations (>2 g/L) produce an inhibitive effect similar to the background of other electrolytes. Studies have shown that a suitable aluminum ion concentration is conducive to the growth of bacteria, while excess concentration can induce changes in the morphological features of cells, combine with some proteins, interact with important enzymes such as nucleic acids and adenosine triphosphate, interfere with a variety of biochemical reactions in the bacteria, and can affect certain cell metabolisms, resulting in their

Corresponding author: Hai Lin E-mail: linhai@ces.ustb.edu.cn

© University of Science and Technology Beijing and Springer-Verlag Berlin Heidelberg 2017

dysfunction [8]. Few studies have analyzed the leaching rule and dissolution kinetics of sericite in chalcopyrite bioleaching.

In this study, a mathematical model of the leaching process was established to determine an effective method for controlling Al^{3+} dissolution and provide a basis for more effective chalcopyrite bioleaching. We examined the leaching rule and dissolution kinetics of sericite in chalcopyrite bioleaching, and also discussed and analyzed the dissolution reaction mechanism and controlling steps in bioleaching.

2. Experimental

2.1. Minerals

The chalcopyrite used in this work was purchased from the Zhejiang University mineral sample factory. The hand-picked chalcopyrite samples were soaked in $4 \text{ mol}\cdot\text{L}^{-1}$ hydrochloric acid for 30 min to clean the surfaces, and then washed three times with distilled water. The chalcopyrite particles were then ground to $<43 \mu\text{m}$ using a porcelain ball mill. The samples were vacuum freeze-dried and sealed with nitrogen. The main chemical composition of the chalcopyrite was 29.38wt% Cu, 30.35wt% Fe, and 35.31wt% S, with a purity of 85.22%. The sericite used was purchased from a company in Hebei Province, China. Its main chemical composition was 63.50wt% SiO_2 , 19.80wt% Al_2O_3 , 6.10wt% K_2O , and 1.34wt% Fe, with a purity of 89.64%. The sericite samples had two particle sizes of $-43 \mu\text{m}$ and $-74 + 43 \mu\text{m}$. Figs. 1 and 2 show the X-ray powder diffraction (XRD) analysis of chalcopyrite and sericite, which shows that the sericite contains a small amount of quartz.

2.2. Microbial strain and culture conditions

Acidithiobacillus ferrooxidans (referred to as *At.f*), isolated from the acid mine water (pH 4.5) of the Daye Copper Mine in Hubei Province, China, was obtained by various

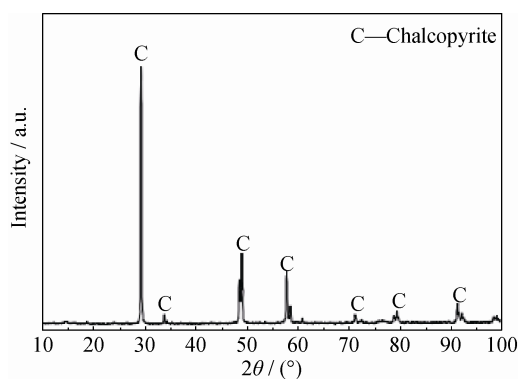


Fig. 1. XRD pattern of chalcopyrite.

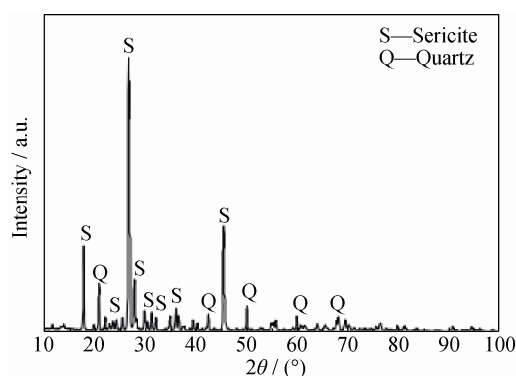


Fig. 2. XRD pattern of sericite.

stages of adaptation and mutation. The optimal conditions for the cultivation of bacteria were set at 30°C , an initial pH value of 2.0, and a rotation speed of 160 r/min [9]. The culture medium, an optimized 9k medium, comprised the following compounds: $(\text{NH}_4)_2\text{SO}_4$, 2.0 g/L; K_2HPO_4 , 0.25 g/L; $\text{MgSO}_4\cdot 7\text{H}_2\text{O}$, 0.25 g/L; KCl, 0.1 g/L; and $\text{FeSO}_4\cdot 7\text{H}_2\text{O}$, 44.2 g/L.

2.3. Experimental method

Bioleaching experiments were performed in 250 mL flasks containing 90 mL optimized 9k medium (pH 2) and 10 mL of inocula. The initial density of the inoculated solution was 1.0×10^7 cell/mL. The concentrations of chalcopyrite and sericite were 0.02 and 0.03 g/mL, respectively. The effects of sericite particle size, dissolved oxygen, and temperature on the dissolution characteristics of sericite and copper extraction were investigated. The flasks were maintained at 30°C and shaken at 160 r/min. The pH value, redox potential, copper ion concentration, and aluminum ion concentration in the leaching solution were determined at certain intervals. The loss of water due to evaporation was compensated with distilled water so that 100 mL was maintained in the flasks. After 48-d leaching, the residues were collected and washed three times with distilled water. Then, after drying, the residues were ready as samples for scanning electron microscopy/energy dispersive spectroscopy (SEM-EDS).

2.4. Analytical methods

The concentration of dissolved copper ions in the leaching solution was analyzed using atomic absorption spectrometry. The concentration of dissolved aluminum ions in the leaching solution was analyzed using an inductively coupled plasma optical emission spectrometer. The surface morphology and chemical composition of the raw minerals and residues after leaching were analyzed using SEM-EDS.

3. Results and discussion

3.1. Dissolution rules of sericite in a leaching system

3.1.1. Effect of particle size on sericite dissolution and copper extraction

The effects of sericite particle size ($-74 + 43 \mu\text{m}$ and $-43 \mu\text{m}$) on Al^{3+} dissolution concentration and the copper extraction rate in the bioleaching system were investigated. The results are shown in Fig. 3.

As shown in Fig. 3(a), the Al^{3+} dissolution concentration increased gradually as the leaching time progressed. A change in sericite particle size affects the Al^{3+} dissolution concentration in the sericite–chalcopyrite leaching system. When the sericite particle size was fine, the Al^{3+} dissolution concentration was higher. After 48-d leaching, the Al^{3+} dissolution con-

centration reached 38.66 mg/L when the sericite particle size was $-43 \mu\text{m}$. However, the Al^{3+} dissolution concentration with the sericite particle size of $-74 + 43 \mu\text{m}$ was only 28.02 mg/L. This may be because finer sericite particles have a larger specific surface area and therefore have a more effective contact surface with the bacteria in the leaching solution. Moreover, the results in Fig. 3(a) demonstrate that the Al^{3+} dissolution concentration rapidly increased in the first 24 d and eventually maintained relative stability; this may be because of the different solution densities around the sericite particle surfaces. During the initial stage of dissolution, ion density in the solution was extremely low, resulting in a high mineral dissolution rate. As the dissolution progressed, the ion density around the mineral particles in the solution increased, thereby reducing the aluminum dissolution rate [10–11].

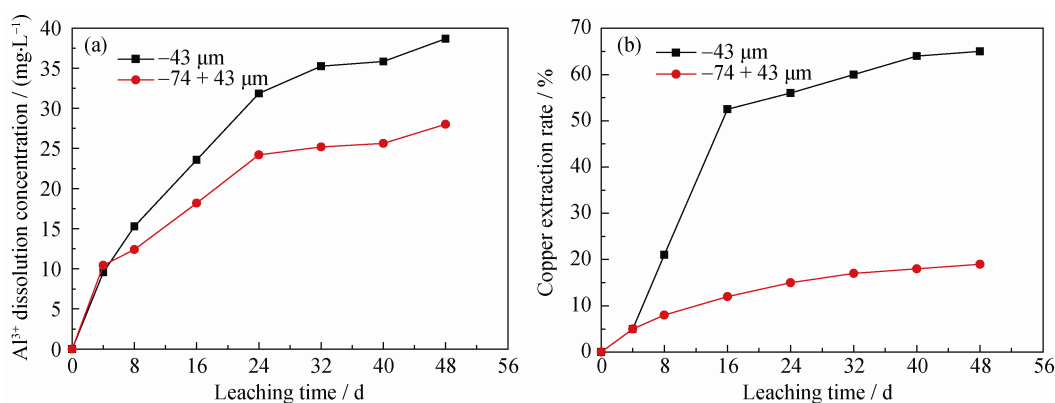


Fig. 3. Effect of particle size on Al^{3+} dissolution concentration (a) and copper extraction rate (b) (rotation speed: 160 r/min; temperature: 30°C).

From Fig. 3(b), it can be seen that copper extraction rapidly increased at first, then slowly increased with increasing the leaching time. Meanwhile, sericite particle size can affect the copper extraction rate in bioleaching. Finer sericite particle size results in a higher rate of copper extraction. When the sericite particle sizes were $-74 + 43 \mu\text{m}$ and $-43 \mu\text{m}$, the copper extraction rates were 66.44% and 19.04% after 48-d leaching, respectively. This could be due to the high Al^{3+} dissolution concentration in the sericite–chalcopyrite leaching system with a sericite particle size of $-43 \mu\text{m}$. A suitable amount of aluminum ions can shorten the lag growth phase of *Atf* bacteria and promote its growth and metabolism, thereby improving copper extraction.

3.1.2. Effect of temperature on sericite dissolution and copper extraction

The sericite particle size used in this work was $-43 \mu\text{m}$. The effects of different leaching temperatures (i.e., 25, 30, and 40°C) on Al^{3+} dissolution concentration and copper extraction rate were studied. The results are shown in Fig. 4.

Fig. 4(a) shows that the Al^{3+} dissolution concentration ra-

pidly increased during the initial period and subsequently became stationary at different leaching temperatures. After 48-d leaching, the Al^{3+} dissolution concentration reached 25.77, 38.66, and 25.89 mg/L at 25, 30, and 40°C, respectively. At 25 and 40°C, the Al^{3+} dissolution speed was relatively high and the Al^{3+} dissolution concentration continued to rapidly increase. In contrast, the Al^{3+} dissolution rate at 30°C was lower during the initial stage; however, it maintained a higher value for a longer period than that at 25 and 40°C. The reason may be that the *Atf* bacteria have higher oxidative activities at 30°C. In general, the dissolution rate of minerals increases with the increase in temperature. Sanna *et al.* [12] discovered that the dissolution rate increases when the temperature increases in acidic or alkaline leaching systems. This is because the increased temperature of the solution can accelerate the diffusion motion of molecules; the inherent mechanism of the effect of temperature on the dissolution rate can be explained by thermodynamics. However, sericite dissolution in a bioleaching system is different from that in an acidic or alkaline solution because of the presence of *Atf* bacteria [13].

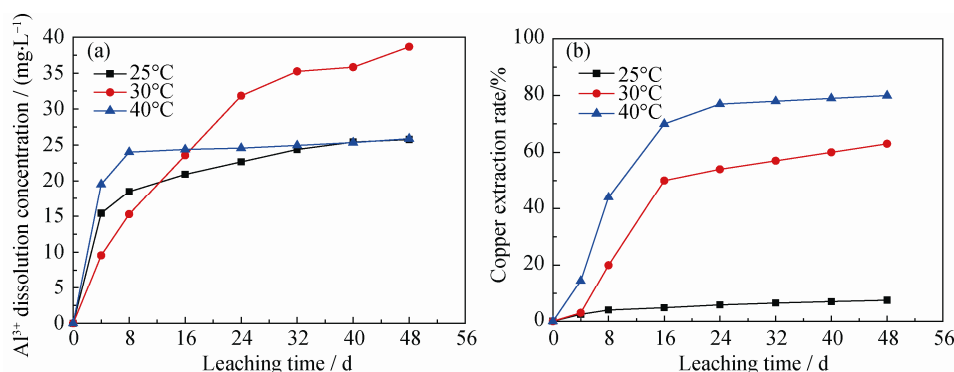


Fig. 4. Effect of temperature on Al³⁺ dissolution concentration (a) and copper extraction rate (b) (rotation speed: 160 r/min; sericite particle size: -43 μm).

Fig. 4(b) shows that leaching temperature is a very significant factor affecting chalcopyrite leaching. The higher the temperature, the higher the copper extraction rate in the bioleaching system. The copper extraction rate reached 81.08% at 40°C after 48-d leaching, which is significantly higher than that at 25 and 30°C. This may be due to the fact that at high temperatures, the crystal lattice of chalcopyrite is easily destroyed by the dual role of the bacteria and temperature; therefore, the copper extraction rate is relatively high. A comparison of the leaching systems at 25 and 30°C shows that copper extraction is significantly different at both temperatures. After 48-d leaching, the copper extraction rate at 30°C increased by approximately 57% compared with that at 25°C. This is because the Al³⁺ dissolution concentration is the highest at 30°C, and a suitable amount of aluminum ions are conducive to copper leaching in a bioleaching system.

3.1.3. Effect of rotation speed on sericite dissolution and copper extraction

The dissolved oxygen is an important parameter for the growth of bacteria, which can be characterized by rotation speed. An appropriate amount of dissolved oxygen can make *At.f* bacteria grow normally. However, a significantly high concentration of dissolved oxygen has a toxic effect on

cells, while significantly low dissolved oxygen cannot satisfy the growth of bacteria [14]. Meanwhile, rotation can suspend the mineral particles in the leaching solution, increasing the contact between sericite and the leaching agent. This can reduce the thickness of the boundary layer on the particle surfaces and the external diffusion resistance, causing more reactants to adsorb onto the mineral surfaces and participate in the reaction per unit time. Accordingly, rotation speeds of 140, 160, and 200 r/min were adopted in this study to assess their effect on the Al³⁺ dissolution concentration and copper extraction rate in the chalcopyrite-sericite bioleaching system. The sericite particle size used for this was -43 μm . The experimental results are shown in Fig. 5.

Fig. 5(a) shows that the effect of rotation speeds on Al³⁺ dissolution from sericite was not obvious. When the rotation speed was 140, 160, and 200 r/min, the Al³⁺ dissolution concentration was 34.93, 38.66, and 35.51 mg/L, respectively, after 48-d leaching. The Al³⁺ concentration at 160 r/min was slightly higher than that at 140 and 200 r/min. At 160 r/min, the *At.f* bacteria were provided with suitable amounts of dissolved oxygen. Fig. 5(b) shows that the copper extraction rate was the highest when the rotation speed was 160 r/min. The reason may be that the Al³⁺ dissolution

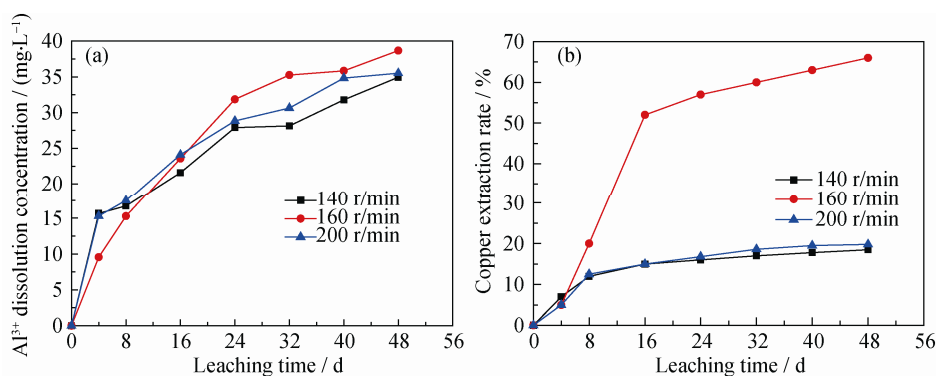


Fig. 5. Effect of rotation speed on Al³⁺ dissolution concentration (a) and copper extraction rate (b) (temperature: 30°C; sericite particle size: -43 μm).

concentration is the highest under a rotation speed of 160 r/min, which is conducive to bacterial adsorption on the chalcopyrite surfaces. Thus, the leaching of copper ions from the chalcopyrite is improved.

3.2. Dissolution kinetics of sericite

The sericite dissolution kinetics in the bioleaching system was explored to determine the rate-controlling step, which may enable specific measures to be taken to change the reaction rate in the process of leaching accordingly.

A leaching model has been proposed with several prototypes, including the particle shrinking core, particle disintegration, porous diffusion, and mixed models. These models have generally been used according to their own specific circumstances and results under different conditions. A widely applied prototype is the particle shrinkage core model [15–18], which can be adopted to describe the process of ore leaching [19]. According to the characteristics of sericite dissolution in a bioleaching system, the classical liquid–solid reaction model (shrinking core model) reasonably describes the dissolution of sericite.

The multiphase reactions of the leaching process generally include adsorption, diffusion, and chemical reaction, and the leaching speed is normally determined by the minimum speed of these. Equilibrium adsorption can be quickly attained. Therefore, the multiphase reaction speed mainly comprises chemical reaction or diffusion. Diffusion control is divided into internal and external.

$$1 - \frac{2}{3}\alpha - (1 - \alpha)^{\frac{2}{3}} = k_1 t \quad (1)$$

$$1 - (1 - \alpha)^{\frac{1}{3}} = k_2 t \quad (2)$$

$$1 - \frac{2}{3}\alpha - (1 - \alpha)^{\frac{2}{3}} + \beta \left[1 - (1 - \alpha)^{\frac{1}{3}} \right] = k_3 t \quad (3)$$

where α is the Al^{3+} dissolution concentration, mg/L; t is the leaching time, d; β is the ratio of diffusion resistance to chemical resistance; and k_1 , k_2 , and k_3 are the reaction rate constants. Eq. (1) is applicable to a diffusion-controlled process through the product layer, Eq. (2) is a chemical reaction controlled at the interface, and Eq. (3) is a mixed controlled process (a combination of surface reaction and diffusion) [20–21].

The Al^{3+} dissolution concentration with different sericite particle sizes in Fig. 3 was fitted by the shrinking core model, which can obtain the best fitting results when the leaching process is divided into two stages (24-d leaching for each stage). All three models were tested, and all the studied data were determined to fit only the relation of the diffusion control in the shrinking core model, $1 - (2/3)\alpha - (1 - \alpha)^{2/3} = k_1 t$.

However, analysis of other kinetic curve plots did not provide a perfect straight line.

The linearization of Fig. 3(a) with Eq. (1) was generated and is shown in Fig. 6. y_1 and y_2 express the different leaching stages of $1 - (2/3)\alpha - (1 - \alpha)^{2/3}$. The rate-controlling step may be changed in the leaching reaction after 24 d.

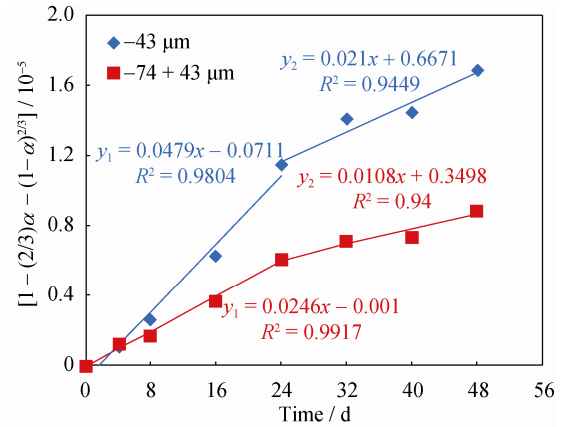


Fig. 6. Diffusion control model of Al^{3+} dissolution under different particle sizes of sericite.

Fig. 6 shows that both curves comprise two lines with line breaks located at the intersection of the 24th day. Results show that the reaction rate constant is associated with particle size and leaching time. The dissolution relation curves under different sericite particle sizes have two lines divided into two stages. These stages are controlled by internal and external diffusion. The external diffusion stage is when the leaching agent passes through the boundary layer and diffuses to the surface of the solid particles and the resultant product diffuses outward from the boundary layer. Meanwhile, the interface diffusion stage is when the leaching agent diffuses to the reaction interface through the solid layer, and the resultant product diffuses through a solid product layer to the boundary layer. In the first stage, the diffusion resistance of the leaching solution was relatively small. This forced the apparent rate constant to be larger, and the reaction proceeded quickly. In the second stage, the surface of sericite was covered with a layer of sediment film, which increased the interface diffusion resistance, hindered the leaching agent and leaching ion diffusion, and decelerated the reaction stage.

The Al^{3+} dissolution concentrations at different rotation speeds, as shown in Fig. 5, were fitted by the shrinking core model, which was determined to perfectly fit the relation of the diffusion control model, $1 - (2/3)\alpha - (1 - \alpha)^{2/3} = k_1 t$. The data were processed with $1 - (2/3)\alpha - (1 - \alpha)^{2/3} = k_1 t$, and the results are shown in Fig. 7.

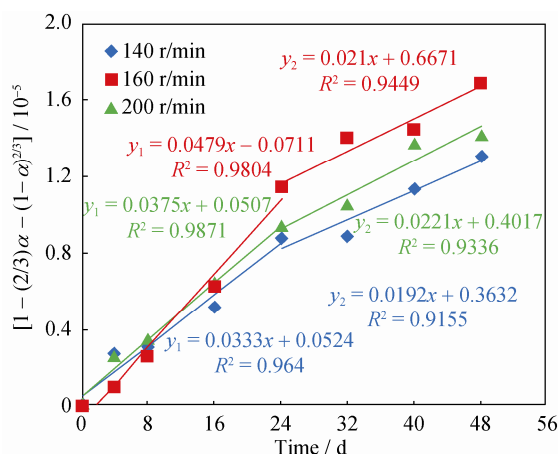


Fig. 7. Diffusion control model of Al^{3+} dissolution at different rotation speeds.

Fig. 7 shows that the diffusion control of the shrinking core model can be used to define sericite dissolution kinetics at different rotation speeds in a chalcopyrite bioleaching system. This also has two lines that intersect on the 24th day. This implies that the dissolution kinetics are divided into two stages that are similar under different particle sizes. Hydrometallurgy dynamics show that in a liquid–solid multiphase leaching reaction, diffusion control can be divided into external and internal. When the control step is external diffusion control, rotation speed significantly influences the leaching rate. However, rotation speed slightly affects the concentration of Al^{3+} dissolved from sericite during bioleaching, as shown in Fig. 5. Therefore, the dissolution reaction controlling step is not external but internal diffusion control. Accordingly, the two stages of sericite stripping diffusion control can be identified as interface diffusion, where the leaching solution diffuses into the interface solution through the solid layer, and the resultant product diffuses through a solid product layer toward the boundary layer.

To further verify if sericite dissolution is suitable for the internal diffusion control model, Al^{3+} concentration at different temperatures, as shown in Fig. 4, was fitted with the shrinking core model. The data were processed with $1 - (2/3)\alpha - (1 - \alpha)^{2/3} = k_1 t$, and the results are shown in Fig. 8.

Fig. 8 shows that although the dissolution kinetics of sericite in the bioleaching system at different temperatures can be explained with the diffusion control model of the shrinking core, they contain two lines that do not intersect at the same point. When the temperatures are 25 and 40°C, the two lines intersect on the 8th day, whereas when the temperature is 30°C, the lines intersect on the 24th day. Fig. 4 shows that Al^{3+} dissolved from sericite does not conform to the general law for minerals in acidic or alkaline leaching. The reaction rate grows exponentially with the increase in temperature.

However, at certain reactant concentrations, the reaction rate of the constant is proportional. Accordingly, sericite dissolution kinetics does not conform to the application of the Arrhenius formula, and the activation energy cannot be obtained. Therefore, the reaction activation energy of sericite dissolution in the system of bioleaching chalcopyrite is no longer discussed using dissolution kinetics.

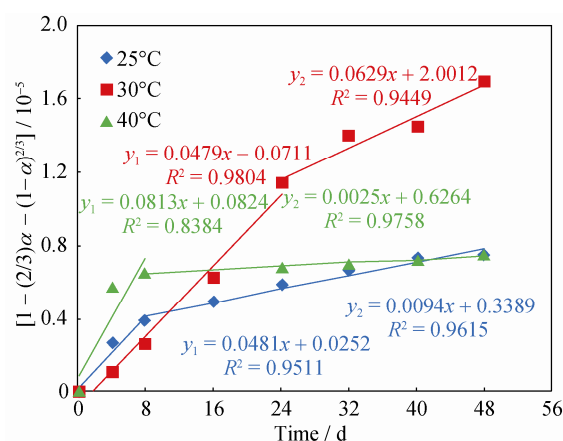


Fig. 8. Diffusion control model of Al^{3+} dissolution at different leaching temperatures.

3.3. SEM-EDS analysis

SEM analysis of sericite before and after leaching is shown in Fig. 9. The edges and corners of the leached residues are a little rougher than those of the raw ore. In particular, the surface of the raw sericite is smooth and angular. After 48-d leaching, edges and surfaces of the sericite are rougher, and they are covered with small particles. These small particles were not obviously observed during the reaction, but several precipitates were adsorbed onto the surfaces. The reason may be that new compounds of ammoniojarosite were generated during the process of bioleaching, and covered the surfaces of chalcopyrite and sericite, thereby hindering chalcopyrite bioleaching to a certain extent.

EDS results (Fig. 10(b)) show that the precipitate on the surface of sericite has K, Al, Fe, and Si peaks. An S peak was also identified. This suggests that sericite not only dissolves, but also adsorbs precipitates from the solution, which causes the surface to be covered by a large amount of precipitate forming a dense film and increases the diffusion resistance of the leaching liquid. The adsorption action also results in diffusion of the leaching solution in the pores, with a certain amount of resistance, and causes the whole dissolution process to be controlled by internal diffusion. When the reaction progresses, the formation of dense films on the surface rapidly increases the diffusion resistance and further increases the inhibition, thereby inhibiting the dissolution of sericite.

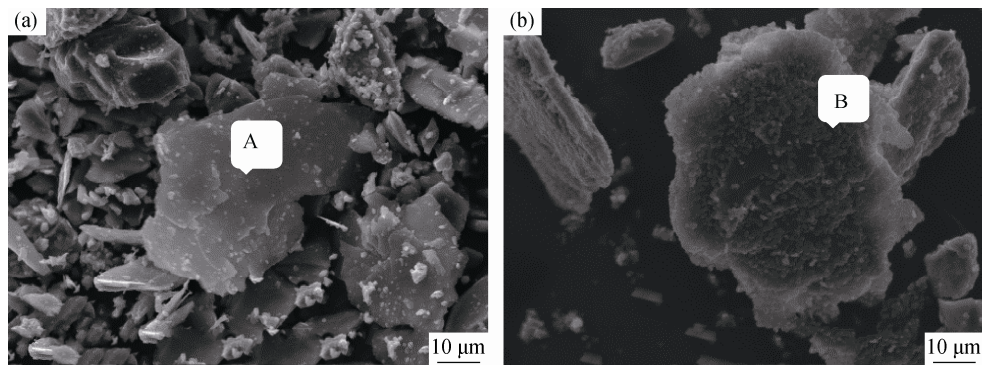


Fig. 9. SEM images of sericite before (a) and after (b) leaching.

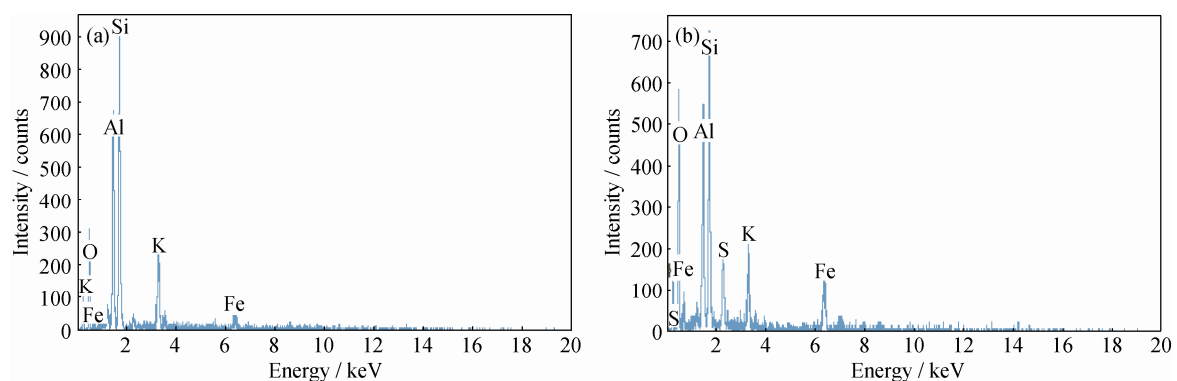


Fig. 10. EDS spectra of sericite before and after leaching: (a) point A in Fig. 9; (b) point B of sediment in Fig. 9.

4. Conclusions

(1) Sericite particle size can affect the Al^{3+} dissolution concentration and copper extraction rates in bioleaching as both were higher when the particle size was finer. The Al^{3+} dissolution concentration at 30°C was higher than that at 25 and 40°C. However, the copper extraction rate was the highest at 40°C, and reached 81.08% after 48-d leaching. The difference in Al^{3+} dissolution concentration at the rotation speeds of 140, 160, and 200 r/min was small. However, the copper extraction rates at 140 and 200 r/min were far lower than that at 160 r/min.

(2) The overall results of this study indicate that the dissolution kinetics of sericite in bioleaching chalcopyrite fit the diffusion control of the shrinking core model, $1 - (2/3)\alpha - (1 - \alpha)^{2/3} = k_1 t$. However, the reaction process was caused by the bioleaching of bacteria, so we cannot use the Arrhenius formula to obtain the reaction activation energy.

(3) The SEM analysis shows that the sericite surface was covered with small particles after 48-d leaching. These particles increased the diffusion resistance of the leaching liquid and hindered the dissolution of sericite, verifying that the dissolution process was affected by internal diffusion control.

Acknowledgements

This work was financially supported by the National Natural Science Foundation of China (No. 51204011) and the Science and Technology Project for the Guidance Teacher of Beijing Excellent Doctoral Dissertation (No. 20121000803).

References

- [1] H.R. Watling, The bioleaching of sulphide minerals with emphasis on copper sulphides: a review, *Hydrometallurgy*, 84(2006), No. 1-2, p. 81.
- [2] Y.G. Guo, P. Huang, W.G. Zhang, X.W. Yuan, F.X. Fan, H.L. Wang, J.S. Liu, and Z.H. Wang, Leaching of heavy metals from Dexing copper mine tailings pond, *Trans. Nonferrous Met. Soc. China*, 23(2013), No. 10, p. 3068.
- [3] X.L. Mo, H. Lin, K.B. Fu, Y.B. Dong, and C.Y. Xu, Effect of sericite on bioleaching of chalcopyrite, *Chin. J. Nonferrous Met.*, 22(2012), No. 5, p. 1475.
- [4] M. Dopson, L. Lövgren, and B. Dan, Silicate mineral dissolution in the presence of acidophilic microorganisms: Implications for heap bioleaching, *Hydrometallurgy*, 96(2009), No. 4, p. 288.
- [5] V. Ochoaherrera, G. León, Q. Banihani, J.A. Field, and R.

- Sierraalvarez, Toxicity of copper(II) ions to microorganisms in biological wastewater treatment systems, *Sci. Total Environ.*, 412-413(2011), No. 13, p. 380.
- [6] J. Fischer, A. Quentmeier, S. Gansel, V. Sabados, and C.G. Friedrich, Inducible aluminium resistance of *Acidiphilium cryptum* and aluminium tolerance of other acidophilic bacteria, *Arch. Microbiol.*, 178(2002), No. 6, p. 554.
- [7] K.R. Blight and D.E. Ralph, Aluminium sulphate and potassium nitrate effects on batch culture of iron oxidising bacteria, *Hydrometallurgy*, 92(2008), No. 3-4, p. 130.
- [8] M. Suwalsky, B. Norris, F. Villena, F. Cuevas, P. Sotomayor, and P. Zatta, Aluminum fluoride affects the structure and functions of cell membranes, *Food Chem. Toxicol.*, 42(2004), No. 6, p. 925.
- [9] Y.B. Dong, H. Lin, H. Wang, X.L. Mo, K.B. Fu, and H.W. Wen, Effects of ultraviolet mutation on bioleaching of low-grade copper tailings, *Miner. Eng.*, 24(2011), No. 8, p. 870.
- [10] D. Bingöl, M. Canbazoglu, and S. Aydoğan, Dissolution kinetics of malachite in ammonia/ammonium carbonate leaching, *Hydrometallurgy*, 76(2005), No. 1-2, p. 55.
- [11] David R. Ely, R. Edwin Garcias, and M. Thommes, Ostwald-Freundlich diffusion-limited dissolution kinetics of nanoparticles, *Powder Technol.*, 257(2014), p. 120.
- [12] A. Sanna, A. Lacinska, M. Styles, and M.M. Maroto-Valer, Silicate rock dissolution by ammonium bisulphate for pH swing mineral CO₂ sequestration, *Fuel Process. Technol.*, 120(2010), No. 4, p. 128.
- [13] A.A. Baba and F.A. Adekola, A study of dissolution kinetics of a Nigerian galena ore in hydrochloric acid, *J. Saudi Chem. Soc.*, 16(2012), No. 4, p. 377.
- [14] M. Gleisner, R.B.H. Jr, and P.C.F. Kockuma, Pyrite oxidation by *Acidithiobacillus ferrooxidans* at various concentrations of dissolved oxygen, *Chem. Geol.*, 225(2006), No. 1-2, p. 16.
- [15] Z.Y. Ding, Z.L. Yin, H.P. Hu, and Q.Y. Chen, Dissolution kinetics of zinc silicate (hemimorphite) in ammoniacal solution, *Hydrometallurgy*, 104(2010), No. 2, p. 201.
- [16] K.C. Liddell, Shrinking core models in hydrometallurgy: What students are not being told about the pseudo-steady approximation, *Hydrometallurgy*, 79(2005), No. 1-2, p. 62.
- [17] R. Salmimies, M. Mannila, J. Kallas, and A. Häkkinen, Acidic dissolution of hematite: kinetic and thermodynamic investigations with oxalic acid, *Int. J. Miner. Process.*, 110-111(2012), p. 121.
- [18] T.J. Hu, G.M. Zeng, and X.Z. Yuan, Leaching kinetics of silver extracted by thiourea from residue in hydrometallurgy of zinc, *Chin. J. Nonferrous Met.*, 11(2001), No. 5, p. 933.
- [19] S.H. Ju, M.T. Tang, S.H. Yang, and Y. Li, Dissolution kinetics of smithsonite ore in ammonium chloride solution, *Hydrometallurgy*, 80(2005), No. 1, p. 67.
- [20] V. Safari, G. Arzpeyma, F. Rashchi, and N. Mostoufi, A shrinking particle-shrinking core model for leaching of a zinc ore containing silica, *Int. J. Miner. Process.*, 93(2009), No. 1, p. 79.
- [21] A. Amiri, G.D. Ingram, A.V. Bekker, I. Livk, and N.E. Maynard, A multi-stage, multi-reaction shrinking core model for self-inhibiting gas-solid reactions, *Adv. Powder Technol.*, 24(2013), No. 4, p. 728.